IEEE Access
Multidisciplinary | Rapid Review | Open Access Journal

Received March 31, 2022, accepted April 14, 2022, date of publication April 18, 2022, date of current version April 27, 2022.

Digital Object Identifier 10.1109/ACCESS.2022.3168679

An Application of the Subwavelength Periodic Microstrip Guard Trace in High-Speed Circuits

CHIA HO WU[1], PEIXUN MA[1], GUOBING ZHOU[1], JIANQI SHEN[2], ZHENYU QIAN[1], LINFANG SHEN[1], HANG ZHANG[1], ZHUOYUAN WANG[3], XIAOLONG WANG[1,4], AND FANG HE[5], (Senior Member, IEEE)

[1]Department of Applied Physics, College of Science, Zhejiang University of Technology, Hangzhou 310023, China
[2]College of Optical Science and Engineering, Zhejiang University, Hangzhou 310058, China
[3]Electronic and Information Engineering College, Ningbo University of Technology, Ningbo 315000, China
[4]Key Laboratory of Quantum Precision Measurement of Zhejiang Province, College of Science, Zhejiang University of Technology, Hangzhou 310023, China
[5]Zhaolong Interconnect Technology Company Ltd., Deqing, Huzhou 313200, China

Corresponding authors: Chia Ho Wu (chwu@zjut.edu.cn) and Peixun Ma (1160177919@qq.com)

This work was supported in part by the National Natural Science Foundation of China under Grant 62075197 and Grant 61875175.

ABSTRACT This paper proposed a kind of guard traces based on a subwavelength periodic structure to reduce the far-end crosstalk (FEXT) of parallel microstrip lines in the PCB. This technology can be used to improve the false triggering and signal transmitting capacity of a multiconductor transmission line circuit system. In order to explore the present novel guard trace effect on isolating electromagnetic interference (EMI), the frequency response of the mutual capacitance and mutual inductance of the overall circuit system was provided and an equivalent circuit model was built. In comparison to the conventional microstrip line for isolating the EMI between parallel microstrip lines, the novel guard trace can efficiently reduce the mutual capacitance and mutual inductance of the overall circuit system. Thus, it is favorable for suppressing the crosstalk between microstrip lines. The *S*-parameters calculation result showed that this kind of subwavelength periodic microstrip guard trace can isolate the EMI between two microstrip lines more effectively. Particularly, the conventional grounded guard trace needs a lot of dense grounded holes, which severely influences the wiring design of various layers of a multilayer circuit board. However, the proposed guard trace requires only one grounded hole, which has little influence on the circuit wiring of each layer of a multilayer printed circuit board. In our experiment, the step function signal of 30 ps rise time was imported into one microstrip line to measure the FEXT of the other microstrip line. It was demonstrated by the measurement result that the subwavelength periodic microstrip guard trace can reduce the FEXT to be below 5% of the transmission signal amplitude and is more flexible in practice. In compliance with the actual demand for a high-speed circuit, three isolation structures were proposed, and their isolation effects on the electromagnetic coupling between microstrip lines were verified individually.

INDEX TERMS Multiconductor transmission lines, crosstalk, guard trace.

I. INTRODUCTION

As the inner capacity of chips for transistors increases greatly, the microstrip lines in the PCBs around chips need to transmit signals at a higher speed. Moreover, as the design of circuit boards develops towards miniaturization, the signals transmitted in the microstrip lines have a higher tendency in attacking adjacent circuits, leading to a severe crosstalk problem. Taking two parallel microstrip lines spaced apart by only a line width as an example, the configuration of strong coupling is formed between microstrip lines. In terms of two 4-inch long parallel conventional microstrip lines, the experimental measurement result showed that almost 50% of energy is coupled to the other microstrip line somewhere about 8 GHz [1]. In terms of the digital signal of 30 ps rise time, the voltage amplitude of the FEXT is higher than 32.5% of input signal [2]. It has been much higher than the tolerant noise margin of 5% of the high-speed digital signal transmission [3]. Therefore, the methods for reducing this type of noise are attracting extensive attention.

The associate editor coordinating the review of this manuscript and approving it for publication was Dušan Grujić.

To overcome excessive electromagnetic noise, the standard textbooks for signal integrity always suggest designers to maintain at least a three times that of the microstrip line width (i.e., 3W rule) for the spacing of two parallel microstrip lines in the case of high-speed signal transmission [3]. The EMI between parallel microstrip lines is always an important research subject. In Refs. [4], [5], the researchers used an electromagnetic numerical method and circuit model for systematic analysis of the EMI between microstrip lines. In order to study the relationship of the intensity of EMI between two parallel microstrip lines to the spacing between microstrip lines, Ref. [6] probed into the variance in electromagnetic coupling strength when the spacing between two microstrip lines changes from one to four times that of the microstrip line width. The numerical calculation result of commercial software and the *S*-parameters obtained by network analyzer verified that the electromagnetic coupling phenomenon between two microstrip lines could be positively reduced by widening the spacing of microstrip lines. However, as the signal frequency increases, or the digital signal rise time shortens, the 3W rule has been unable to meet the requirement of a high-speed circuit. For example, when a step function signal of 30 ps rise time is fed into one port of two parallel microstrip lines spaced apart by 3W, the other microstrip line perceives a FEXT with input signal amplitude of 10.2%. Obviously, in the higher frequency or high-speed circuit, the 3W rule cannot meet the requirement for EMI noise reduction at all. Clearly, if the spacing of two microstrip lines is changed to four times that of the line width, miniaturization of circuit area encounters a bottleneck, thus increasing the difficulties in PCB wiring for circuit designers. Therefore, it is urgent to seek for a more effective way to obstruct EMI between two parallel microstrip lines. Two coupled parallel microstrip lines have two eigen-modes, i.e., odd and even modes, and the crosstalk between two parallel microstrip lines is derived from different phase velocities of odd and even modes. The phase velocity of odd or even modes can be determined by their corresponding capacitance and inductance. Therefore, the crosstalk can be reduced by modifying the capacitance and inductance of odd and even modes of coupled microstrip lines. In the literature, Wang *et al.* [7] bridged a series of decoupling capacitors over two microstrip lines to reduce the phase velocity difference between odd and even modes, so as to suppress FEXT.

On the other hand, the scheme that a guard trace in between two parallel microstrip lines is introduced in order to isolate FEXT and near-end crosstalk (NEXT) is the mainstream technology at present. In this topic, the authors of Ref. [8] used the finite difference time domain (FDTD) numerical method to analyze the influence of putting a microstrip shielding wire in nonuniform width in between two parallel microstrip lines on crosstalk. At present, the most frequently used technology for isolating EMI of commercial products is to place a grounded guard trace between two microstrip lines. This type of grounded guard trace is extensively applied in high frequency and high-speed circuit products. The researchers utilized electromagnetic numerical methods and equivalent circuits to explore many important features of grounded guard trace [9]–[15]. The grounded guard trace contains a series of metallic grounded holes inside microstrip lines for isolating crosstalk. For example, Ladd *et al.* [9] used 2D finite element method, and extracted the mutual capacitance and mutual inductance from time-invariant Maxwell equations to study how much the grounded guard trace isolated EMI. Lin *et al.* [12] substituted a straight grounded guard trace with serpentine warp architecture, and used a network analyzer to measure the suppression effect of grounded guard trace on the EMI between two parallel microstrips. Suntives *et al.* [13] studied the relationship between the spacing of metal hollow cylinders in grounded guard trace and *S*-parameters resonant coupling in the printed circuit board. According to the software simulation data, the resonant coupling of *S*-parameters can be reduced by shortening the spacing of metal hollow cylinders. This indicates that the grounded guard trace between two coupled parallel microstrip lines can induce high density metal hollow cylinders on the substrate. As this phenomenon interferes with the route planning of various layers of multilayer circuit board, there exists serious problems in the use of grounded guard trace. Moreover, the grounded guard trace does not work well in higher frequency bands [2].

A physical phenomenon that seems to be unrelated to high-speed signal transmission may provide a brand new proposal to overcome the problem of crosstalk between the microstrip lines. In optical frequency ranges, the periodic structure has been used for designing optical filter, reflector or antenna for a long time [16]–[19]. However, Pendry proposed an idea that an etched subwavelength periodic array pore structures on the metal surface could have electromagnetic modes confined to the conductor surface [20]. On the other hand, Lee *et al.* [21] suggested sandwiching two periodic microstrip lines in each other to increase the mutual capacitance ratio of two microstrip lines (ratio of mutual capacitance to self-capacitance), and to eliminate FEXT. Though the periodic microstrip lines that are embedded into each other for eliminating EMI has a good effect on suppressing FEXT, it also increases NEXT obviously. This wiring method is unlikely to be directly applied to differential microstrip lines for transmitting high-speed signals. Afterwards, some researcher applied a subwavelength periodic structure to the edge of conventional microstrip lines, and found that the intensity of electromagnetic field could be confined in the microstrip lines [1]. The periodic structure is etched at the microstrip line edge, usually used as low-pass filters or a tool for changing the characteristic impedance of microstrip lines. However, when the lattice constant of periodic structure is much smaller than the wavelength, the microstrip line can have a sufficient transmission bandwidth. Several types of subwavelength microstrip lines were proposed for reducing the crosstalk between the microstrip lines [22]–[24]. Based on these schemes, Wu *et al.* [25] introduced a subwavelength periodic structure into the conventional differential microstrip

lines of high-speed circuits, where the experimental results [25] showed that the common mode and crosstalk effects in such a differential circuit can be suppressed simultaneously. In order to provide a circuit model of subwavelength periodic differential microstrip lines, the authors of Ref. [26] suggested a method for extracting the circuit parameters of such differential periodic microstrip lines. The circuit model can be combined with active devices and can use SPICE simulator to simulate the differential circuit system. Alternatively, a discontinuous protective line has also been introduced in the middle of the two subwavelength periodic microstrip lines to change the mutual capacitance and mutual inductance for eliminating the far-end crosstalk in the microwave and millimeter wave frequency bands [27]. It is obvious that the electromagnetic interaction on conventional microstrip lines can be mitigated by importing the subwavelength periodic structure into the edge of microstrip lines. However, there is a problem in the application of these subwavelength periodic microstrip structures: specifically, it is difficult to obtain the circuit parameters and characteristic impedance of this type of microstrip lines, and the previously published works seldom relate to the calculation and measurement of characteristic impedance of this type of microstrip structure. In the literature, it was shown that the subwavelength periodic microstrip lines has relatively high reflection coefficient, meaning the characteristic impedance deviates from 50 Ω. Moreover, the variation of characteristic impedance with frequency is relatively apparent, and so it is unlikely to realize the impedance matching with the conventional microstrip line broadband. If the wiring in the circuit system cannot tolerate excessive reflections, it is necessary to choose a new scheme to suppress crosstalk. However, the electromagnetic coupling effect between a subwavelength periodic microstrip line and a conventional microstrip line can be reduced efficiently. Therefore, we suggest a brand new idea that the subwavelength periodic microstrip line is still applicable to high-speed circuits, which is to say, the subwavelength periodic microstrip line is used to isolate the EMI between two conventional microstrip lines for transmitting signals.

The present paper is organized as follows: In Part 1 of this paper, three guard traces based on subwavelength periodic microstrip lines were proposed. As the guard trace includes 1 or 2 resistors, in order to make the selected resistors match the characteristic impedance of an applied subwavelength periodic microstrip line, the circuit parameters of subwavelength periodic microstrip lines were calculated by using the basic definitions in electromagnetics, and the relationship between characteristic impedance and frequency was obtained. The circuit parameters (including the mutual capacitance and mutual inductance) of overall circuit system were determined numerically, and the circuit models of two parallel microstrip lines and a subwavelength periodic microstrip guard trace were built. These accurate models could be combined with active devices, and the overall circuit system can be well simulated by using SPICE simulator. On the other hand, the full-wave numerical method was used for numerical simulation of the circuit system with a subwavelength periodic microstrip guard trace to determine the isolation effect of a subwavelength periodic microstrip guard trace on a frequency domain signal. In Part 2, the network analyzer and a time-domain reflectometer (TDR) were used to measure the isolation effect of the subwavelength periodic microstrip guard traces on EMI in an actual circuit.

II. THEORETICAL ANALYSIS

The electromagnetic field can be confined effectively and the EMI with adjacent microstrip lines can be isolated by etching the subwavelength periodic structure at the edge of microstrip line. This is apparently an important innovation. However, when the subwavelength periodic microstrip line is used to transmit electromagnetic signals, several problems should be taken into account. Firstly, as the microstrip line has a periodic structure, the relationship between characteristic impedance and frequency cannot be obtained with quasistatic method. Secondly, the subwavelength periodic microstrip line is unlikely to perform impedance matching with the conventional microstrip line, which leads to strong reflected waves. Thirdly, when the signals are being transmitted through the subwavelength periodic microstrip line, the jitter effect of S-parameters with frequency is likely to occur. However, it is observed in Refs. [1] and [2] that the subwavelength periodic microstrip line can efficiently suppress the interaction with a conventional microstrip line. In order to avoid the three above problems, the present study employed a subwavelength periodic microstrip line to isolate the signal interference between two conventional microstrip lines. High-speed digital signals are still transmitted through the conventional microstrip line, but the subwavelength periodic microstrip line acts as the isolation structure for electromagnetic signal interference source, i.e., it does not transmit any electromagnetic signals. As an isolation structure, its schematic diagram is shown in Fig. 1 (a)-(c). The EMI between microstrip lines is isolated by a bilateral subwavelength periodic microstrip line (BSPML). The edge of microstrip line includes the subwavelength periodic structure, where the lattice constant is d, the depth of slot is b, the width of slot is a, the thickness of metal layer is t, the dielectric constant of substrate under the microstrip structure is ϵ_r, and the height is h. To make the subwavelength periodic microstrip guard trace give rise to a dramatic isolation effect, the lattice constant of periodic structure should be designed in subwavelength scale, i.e., $d \ll \lambda$, where λ is the signal wavelength. Alternatively, a quite strict mandatory requirement is $d < \lambda/4$. The main purpose of this study is to analyze the ability of the four type microstrip isolation structures to decouple an EMI. In order to validate our conception with experimental results, an RO4003 circuit board is used, where the thickness of the metal layer is $t = 0.0175$ mm, the thickness of dielectric medium is $d = 0.508$ mm, and the dielectric constant is $\epsilon_r = 3.37$. To enable the conventional microstrip line and SMA to perform perfect impedance matching, the

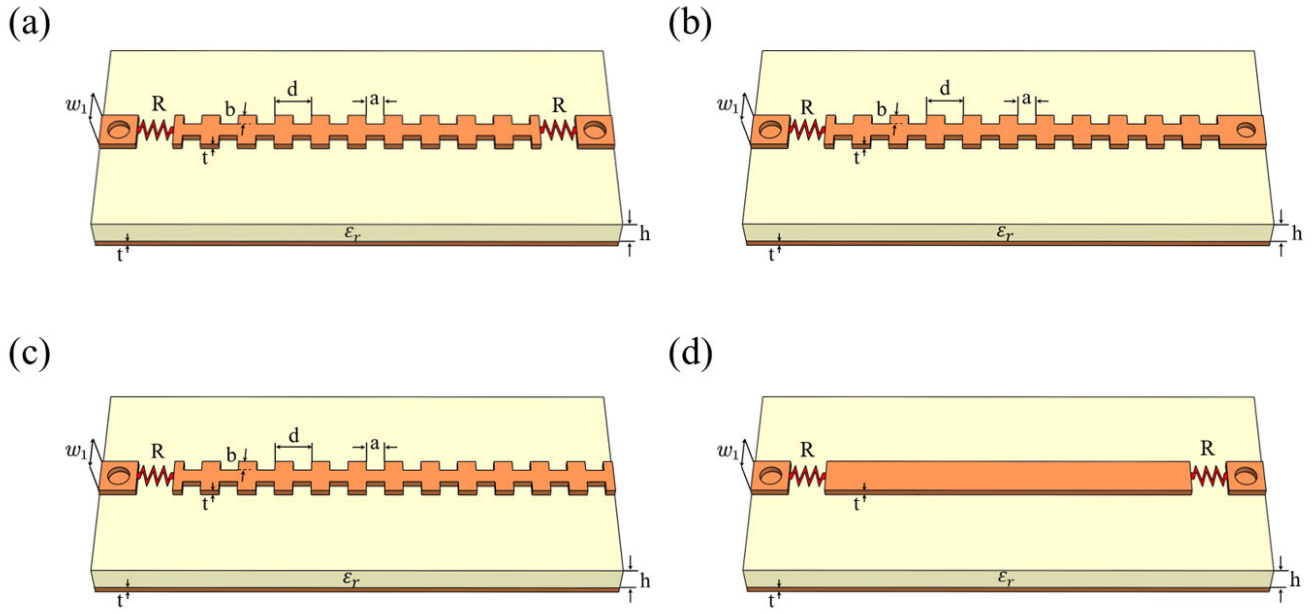

FIGURE 1. The schematic diagram of subwavelength periodic microstrip guard trace structure. In panel (a) is a subwavelength periodic microstrip guard trace with its front and back ends connected to resistors; In panel (b) is a subwavelength periodic microstrip guard trace with one end connected to a resistor and the other end grounded; In panel (c) is a subwavelength periodic microstrip guard trace with one end connected to a resistor and the other end unconnected to any components; In panel (d) is a conventional microstrip guard trace with its front and back ends connected to resistors.

width of the microstrip line is set as $w_1 = 1.14$ mm. Such a setting ensures that the S_{11} measured by the SMA connector can be smaller than -30 dB in a low frequency range. The lattice constant d of BSPML as an isolation structure is 0.5 mm, 1.0 mm, and 2.0 mm, respectively. The depth of slot $b = 0.3\ w_1$ and the width of slot $a = 0.5\ d$. The depth and width of the slot can be changed as required if the circuit manufacture allows in practice. Fig. 1 (a) shows that each of the front and back ends of the microstrip isolation structure is provided with an impedance matching resistor, and is connected to the current return path via a metal hollow cylinders. This subwavelength periodic microstrip line does not transmit any signals, meaning that it is not connected to any signal sources, or selected as a port of input and output signals. The microstrip line for isolating EMI and the microstrip line for transmitting signals have completely different effects. The commercial grounded guard trace is usually formed by importing a series of metal cylinders connected to the current return path into the isolation microstrip lines. It is noted that the metal cylinders are disposed only on the front and back ends of guard trace and there are not any grounded holes in the middle region. If this isolation structure is directly used for isolating two signal lines, the isolation microstrip and current return path form a resonant cavity, and it was pointed out in Ref. [13] that the isolation effect shows the resonance in the transmission coefficient. Because of such a resonance effect, the conventional microstrip line cannot transmit complete digital signals. To avoid the resonance effect between the two conventional microstrip lines when the third microstrip line serves as an isolating line, the front and back ends of subwavelength periodic microstrip line are not directly connected to the current return path, but to the resistor matching the impedance of subwavelength periodic microstrip line, and then connected to two metal cylinders respectively. However, in many practical applications, sometimes the guard trace is only allowed to connect one resistor (e.g., used in the circuit nearby adapter), so the guard microstrip line connected to only one resistor is considered, as shown in Fig. 1 (b) and (c). The microstrip structure in Fig. 1 (b) only connects a grounded resistor to one end of the subwavelength microstrip line, and the other end is a metal cylinder. Such a metal cylinder can be connected to the current return path, or connected to nothing. In Fig.1(c), the two ends of the resistor are connected to the microstrip line and an end of the metal cylinder, respectively, and the other end of the metal cylinder is connected to the current return path. The other end of the microstrip line is connected to a capacitor, or connected to nothing. Additionally, as a control group, a conventional microstrip line to isolate the EMI of two microstrip lines, as shown in Fig. 1 (d), is utilized.

To make the magnitude of resistor accurately perform impedance matching with the subwavelength periodic microstrip line, such a magnitude of resistor that is connected to the subwavelength microstrip line can be obtained by calculating the characteristic impedance of the subwavelength periodic microstrip line. Under the condition of quasi-TEM, the capacitance per unit length of the microstrip line can be obtained by the Gauss law. Firstly, the conductor surface is integrated in order to derive the charge accumulated per unit

length of the microstrip line [28]

$$\oint_{S_1} \vec{D} \cdot d\vec{s} = Q \tag{1}$$

where the range of integration S_1 is the curved surface surrounding the microstrip line. The electric field integral between the microstrip line and the current return path is calculated for obtaining the potential difference

$$-\int_0^h \vec{E} \cdot d\vec{l} = V \tag{2}$$

Therefore, the capacitance of microstrip line can be expressed as

$$C = Q/V \tag{3}$$

The inductance can be derived from the ratio of the microstrip line magnetic flux linkage to the current I

$$L = \Phi/I \tag{4}$$

where Φ is the microstrip line magnetic flux linkage. This linkage can be deduced from the flux integration of magnetic flux density

$$\Phi = \iint_{S_2} \vec{B} \cdot d\vec{s} \tag{5}$$

Here, the range of integration S_2 is the magnetic flux linkage surface. The current can be obtained by Ampere's law

$$\oint_C \vec{H} \cdot d\vec{l} = I \tag{6}$$

To calculate the ohmic loss of microstrip line, the most frequently used perturbation method for the conventional waveguide is employed aiming at the magnitude R of the resistance of the microstrip line. The average wasted power of each unit cell conductor in the periodic structure is calculated by the magnetic field component of the electromagnetic wave [29]

$$P_{av} = \frac{1}{2} R_s \iint_s \left|\vec{H}_t\right|^2 ds \tag{7}$$

where R_s is the surface resistance of the metallic conductor and $\vec{H}_t$ is the magnetic field intensity component on the conductor surface. The resistor as a metallic conductor can be expressed as follows

$$P_{av} = \frac{1}{2} R I^2 \tag{8}$$

As the dielectric materials have leakage current, the conductance G can be derived from the capacitance of the microstrip line [3]

$$G = \omega \tan(\delta) C \tag{9}$$

By using the circuit parameters, including $RLGC$, the characteristic impedance of the microstrip line can be calculated. Since the metal ohmic loss and dielectric leakage current

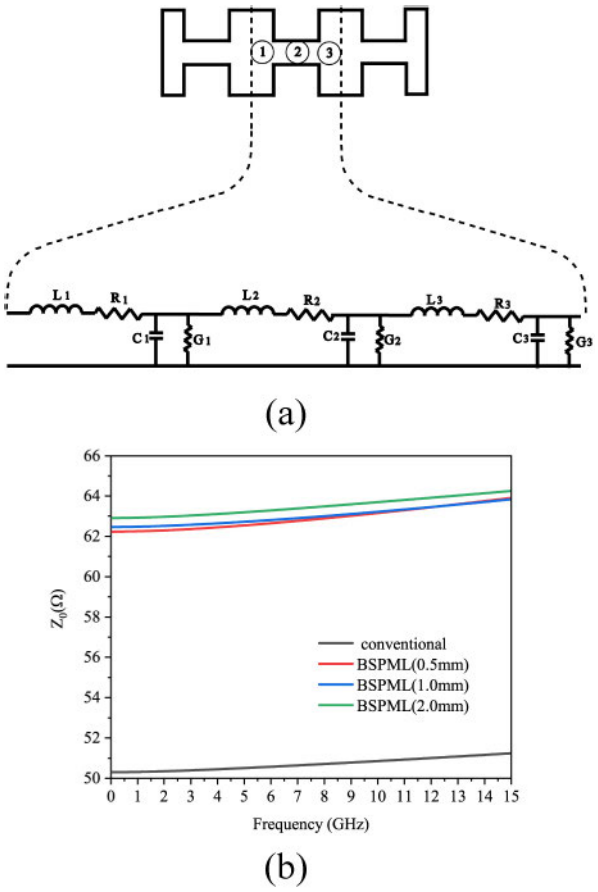

FIGURE 2. Equivalent circuit and characteristic impedance of subwavelength periodic microstrip line. In panel (a) is an equivalent circuit of a unit cell of subwavelength periodic microstrip line; In panel (b) is the relationship between the characteristic impedance of subwavelength periodic microstrip line and the frequency.

in the low frequency range is very low, the characteristic impedance can be expressed as

$$Z_0 = \sqrt{\frac{L}{C}} \tag{10}$$

The extraction of circuit parameters of one subwavelength microstrip line is executed in COMSOL software. Each unit cell and equivalent circuit of subwavelength periodic microstrip line are shown in Fig. 2 (a). The behavior of variation of the characteristic impedance of subwavelength periodic microstrip line responding to the frequency is plotted in Fig. 2 (b). For a conventional microstrip line, the characteristic impedance $Z_0 = 50.306\ \Omega$ at 0.05 GHz and the characteristic impedance of subwavelength periodic microstrip line of lattice constant $d = 0.5$ mm at 0.05 GHz is $Z_0 = 62.227\ \Omega$. When the subwavelength periodic structure is imported into the edge of microstrip line, the characteristic impedance increases rapidly with frequency. The subwavelength periodic microstrip line connected resistance value can be chosen as the characteristic impedance of the present microstrip line in the isolation line in Fig. 1. For the quantitative analysis of the electromagnetic field decoupling effect of subwavelength periodic microstrip guard trace on two conventional

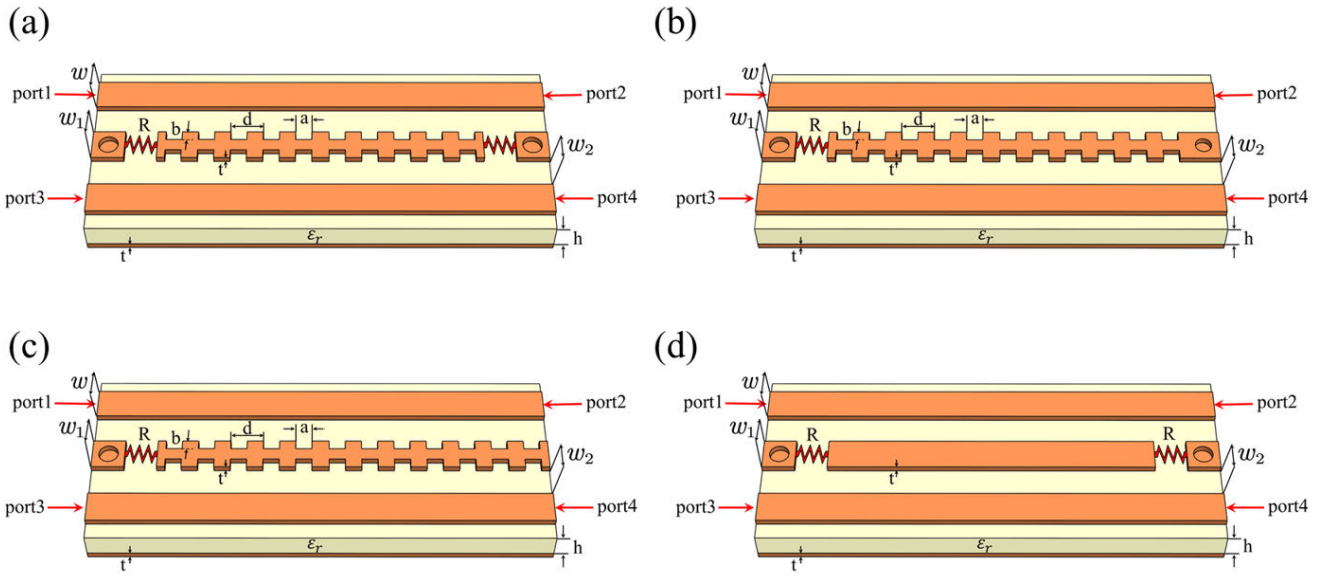

FIGURE 3. Parallel microstrip lines using a guard trace to isolate electromagnetic interference. In panel (a), there is a subwavelength periodic microstrip guard trace with its front and back ends connected to resistors placed in between two parallel microstrip lines; In panel (b) is the subwavelength periodic microstrip guard trace with one end connected to a resistor and the other end grounded placed in between two parallel microstrip lines; In panel (c), the subwavelength periodic microstrip guard trace has one end connected to a resistor and the other end unconnected to any components placed in between two parallel microstrip lines; In panel (d), there is a microstrip guard trace with both ends connected to resistors placed in between two parallel microstrip lines.

microstrip lines, the circuit structure in Fig. 3 needs to be considered.

In Fig. 3 (a), a subwavelength periodic microstrip line has its front and back ends connected to resistors as a guard trace in the parallel microstrip line circuit. Fig. 3 (b) shows the guard trace of the subwavelength periodic microstrip line with one end connected to a resistor and the other end grounded by a metal cylinder. In Fig. 3 (c) is a subwavelength periodic microstrip guard trace with one end connected to a resistor and the other end unconnected to any components. In Fig. 3 (d), there is a circuit system, in which a conventional microstrip line is utilized as a guard trace. By making use of a circuit model to analyze the interaction of conventional microstrip line and subwavelength periodic microstrip guard trace, the mutual capacitance and mutual inductance of the overall circuit system should be calculated. For the circuit system of multiconductor transmission line, in the approximation of quasi-TEM, the mutual capacitance and mutual inductance of all microstrip lines are calculated, where the circuit system in Fig. 3 (a) is taken as an example. In the capacitance matrix, the relationships between the charge Q accumulated on the microstrip line surface and the potential V are expressed as follows

$$Q_1 = C_{11}V_1 + C_{12}(V_1 - V_2) + C_{13}(V_1 - V_3) \quad (11)$$
$$Q_2 = C_{22}V_2 + C_{21}(V_2 - V_1) + C_{23}(V_2 - V_3) \quad (12)$$
$$Q_3 = C_{33}V_3 + C_{31}(V_3 - V_1) + C_{32}(V_3 - V_2) \quad (13)$$

where C_{11}, C_{22}, and C_{33} are the self-capacitances of the microstrip lines and $C_{ij}(i \neq j)$ denote the mutual capacitances between two microstrip lines.

Since the charge accumulated Q_i and the voltage V_i per unit length of each microstrip line are known, each element in the capacitance matrix can be computed simultaneously by solving the above equations. The relationships between the current I and the microstrip line magnetic flux linkage Φ can be observed in the inductance matrix, expressed as follows

$$\Phi_1 = L_{11}I_1 + L_{12}I_2 + L_{13}I_3 \quad (14)$$
$$\Phi_2 = L_{21}I_1 + L_{22}I_2 + L_{23}I_3 \quad (15)$$
$$\Phi_3 = L_{31}I_1 + L_{32}I_2 + L_{33}I_3 \quad (16)$$

where L_{11}, L_{22}, and L_{33} denote the self-inductances of the microstrip lines, and $L_{ij}(i \neq j)$ are the mutual inductances between two microstrip lines. The current I_i transmitted through each microstrip line and the microstrip line magnetic flux linkage Φ_i are known. Then each element of the inductance matrix can be computed. The schematic diagram of the circuit model of the system with the guard trace is shown in Fig. 4 (a). In the case currently discussed, the line width w of the conventional microstrip line, the spacing w_1 between the microstrip line and the guard trace, and the line width w_2 of the guard trace are chosen as the same values. The numerical result for the behavior of dispersion of mutual capacitance C_{12} and mutual inductance L_{12} of the guard trace isolated circuit system is given in Fig. 4 (b) and (c). In the current example, the line width w and w_1 of the conventional microstrip line and the microstrip guard trace, respectively, are selected to be the same as the spacing w_2 between the microstrip line and the guard trace, that is $w = w_1 = w_2$. The mutual capacitance C_{12} between the subwavelength periodic microstrip guard trace and the conventional microstrip line

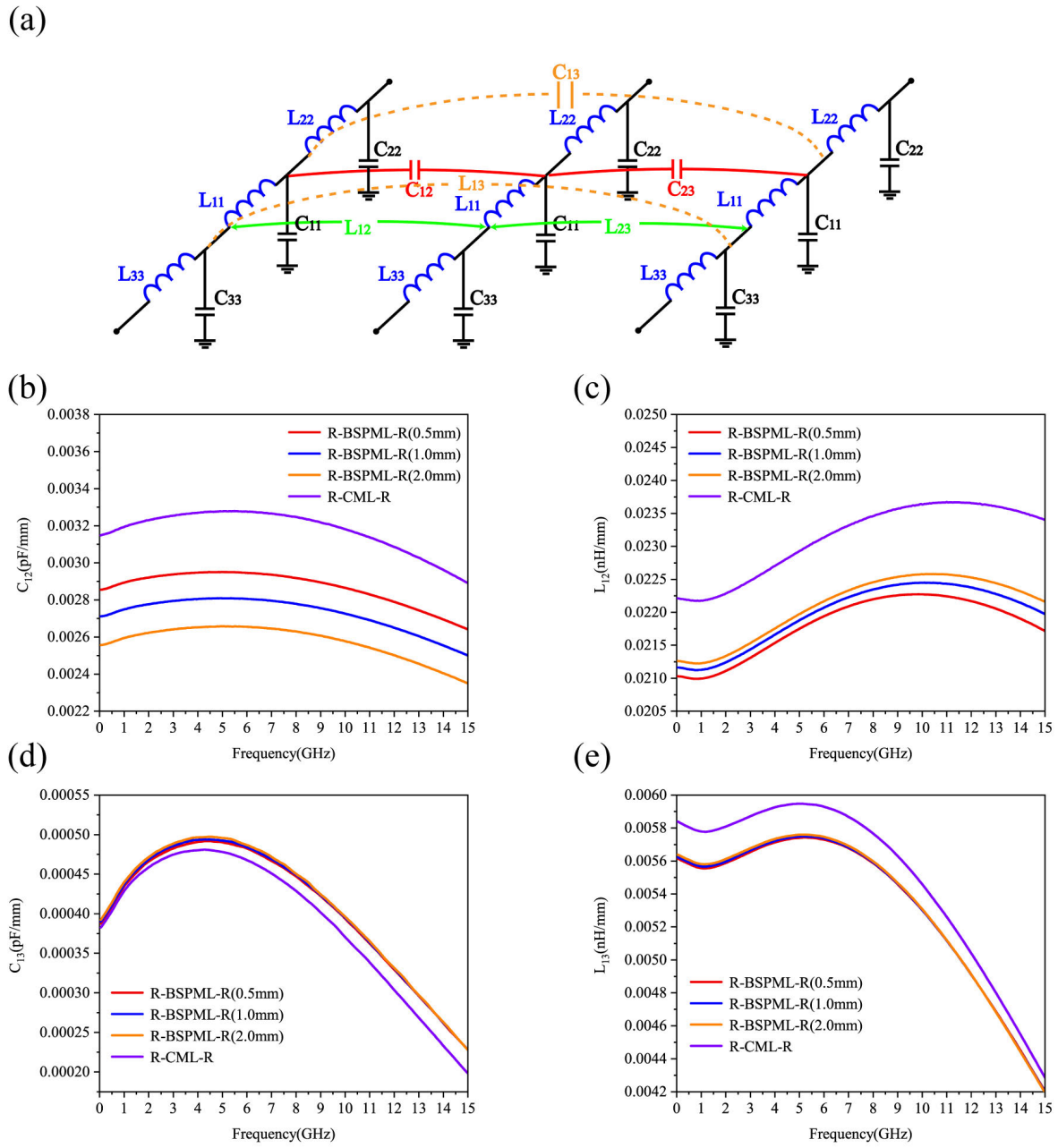

FIGURE 4. The circuit model of parallel microstrip lines with a guard trace in (a) and the mutual capacitance and mutual inductance of circuit systems in (b)-(e). The relationship between the mutual capacitance C_{12} and the frequency is shown in panel (b); In panel (c) is the relationship between the mutual inductance L_{12} and the frequency; The relations of the mutual capacitance C_{13} and the mutual inductance L_{13} to the frequency are given in panels (d) and (e), respectively.

increases slowly with the frequency when the frequency is less than 5 GHz, but it decreases when the frequency goes beyond 5 GHz. In Fig. 4 (b), it is also indicated that the value of C_{12} decreases as the lattice constant d increases. It is shown that the circuit system using the conventional microstrip line as the guard trace has its maximum mutual capacitance C_{12}. In Fig. 4 (c), it can be pointed out that the circuit system using conventional microstrip line for isolation has the maximum mutual inductance L_{12}. The mutual inductance L_{12} between the conventional microstrip line and the subwavelength periodic microstrip guard trace decreases when the lattice constant d becomes smaller. After the subwavelength periodic structure has been etched at the edge of a microstrip line, the mutual capacitance and mutual inductance of adjacent microstrip lines will decrease simultaneously. In Fig. 4 (d) and (e), our numerical simulation presents the dispersion behavior of the mutual capacitance C_{13} and mutual inductance L_{13} of circuit system. Apparently, when

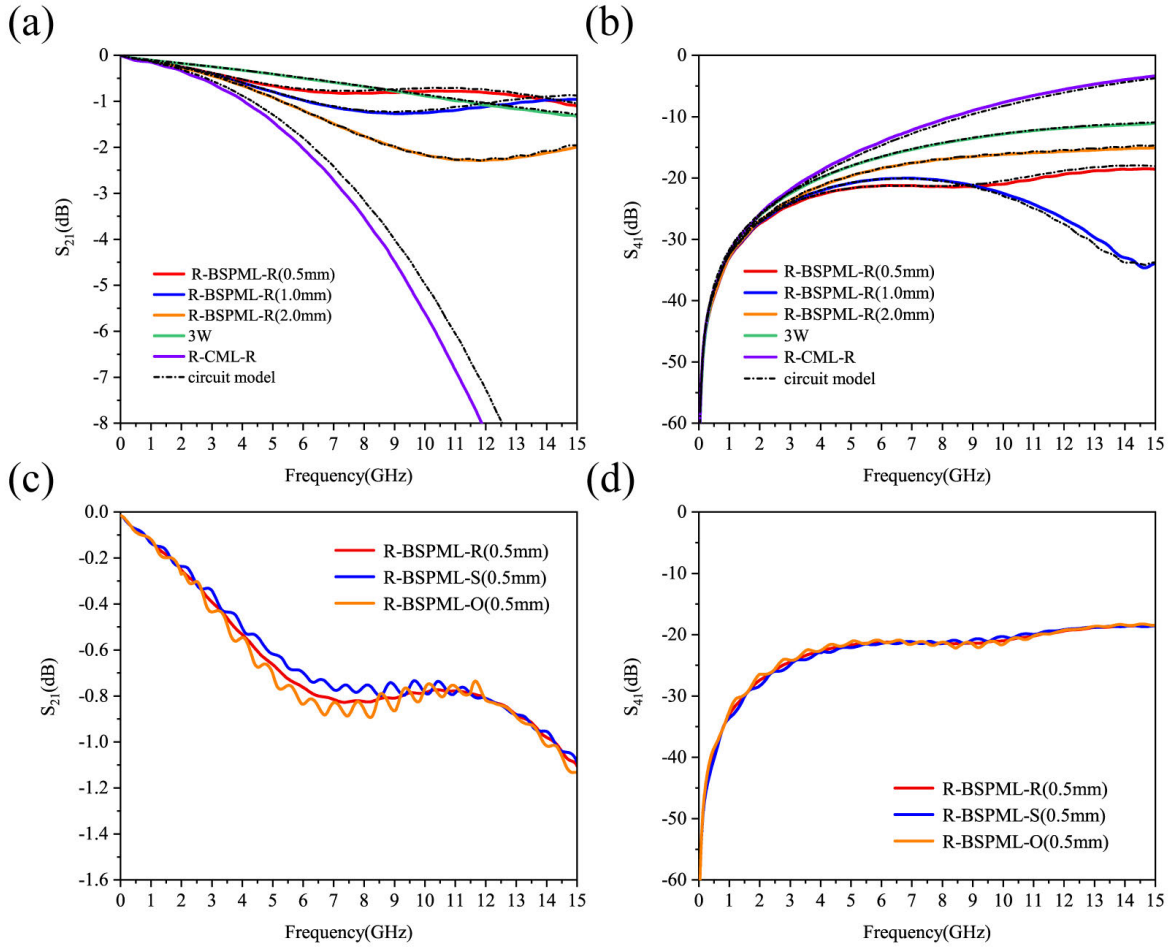

FIGURE 5. The numerical results of influence of the guard trace on the *S*-parameter of parallel microstrip lines. The S_{21} and S_{41} of parallel microstrip lines with isolation of guard trace are given in panel (b) and (c), respectively; The influence of the subwavelength periodic guard trace with only one end connected to a resistor on the S_{21} and S_{41} of parallel microstrip lines is presented in (c) and (d), respectively.

the conventional microstrip line is used as a guard trace, the mutual capacitance C_{13} is smaller but slightly different from the other types of guard traces. The conventional microstrip guard trace as shown in Fig. 3 (d) has a mutual inductance L_{13} larger than that of the subwavelength periodic microstrip guard trace as shown in Fig. 3 (a)-(c). Since the circuit system in Fig. 4 (a) is of left-right symmetry in its structure, one can have the relations of mutual capacitance $C_{ij} = C_{ji}$ and mutual inductance $L_{ij} = L_{ji}$. Then by using the relevant circuit parameters (R, L, G, C), the S-parameters can be calculated within the framework of the circuit model, and in order to validate the rationality of these relevant circuit parameters, the obtained S-parameter will be compared with the full-wave numerical result. In Fig. 5 we numerically calculate the S-parameters in the circuit model for five isolating methods. The length of all microstrip lines is chosen as 10 cm during numerical calculation. The full-wave numerical result and circuit model calculation of S-parameters are presented by solid line and black dot-dash line, respectively. In Fig. 5 (a) it is shown that the S_{21} parameter of the two microstrip lines, of which the spacing is chosen as three times that of the microstrip line width, almost linearly decreases from 0 dB to -1.33 dB at 15 GHz. For the two parallel microstrip lines that is isolated by a subwavelength periodic microstrip guard trace of lattice constant $d = 0.5$ mm, the value of S_{21} decreases faster than the aforementioned two microstrip lines.

However, this value is larger than that of the two parallel microstrip lines mentioned above after 9 GHz. This, therefore, means that the subwavelength periodic microstrip line can exhibit a better isolation effect in high frequency band, e.g., $S_{21} = -1.1056$ dB at 15 GHz. Fig. 5 (b) shows the trend of variation of numerical result of S_{41} with frequency, i.e., the far-end crosstalk of frequency domain. In the case of two microstrip lines spaced apart by three times that of the line width, the value of S_{41} is -11.116 dB at 15 GHz. When the subwavelength periodic microstrip line with lattice constant $d = 1.0$ mm plays the role of an isolation structure, the value of S_{41} is -33.971 dB when the frequency is 15 GHz. The maximum value of the frequency-domain far-end crosstalk S_{41} of the circuit isolated by the subwavelength periodic

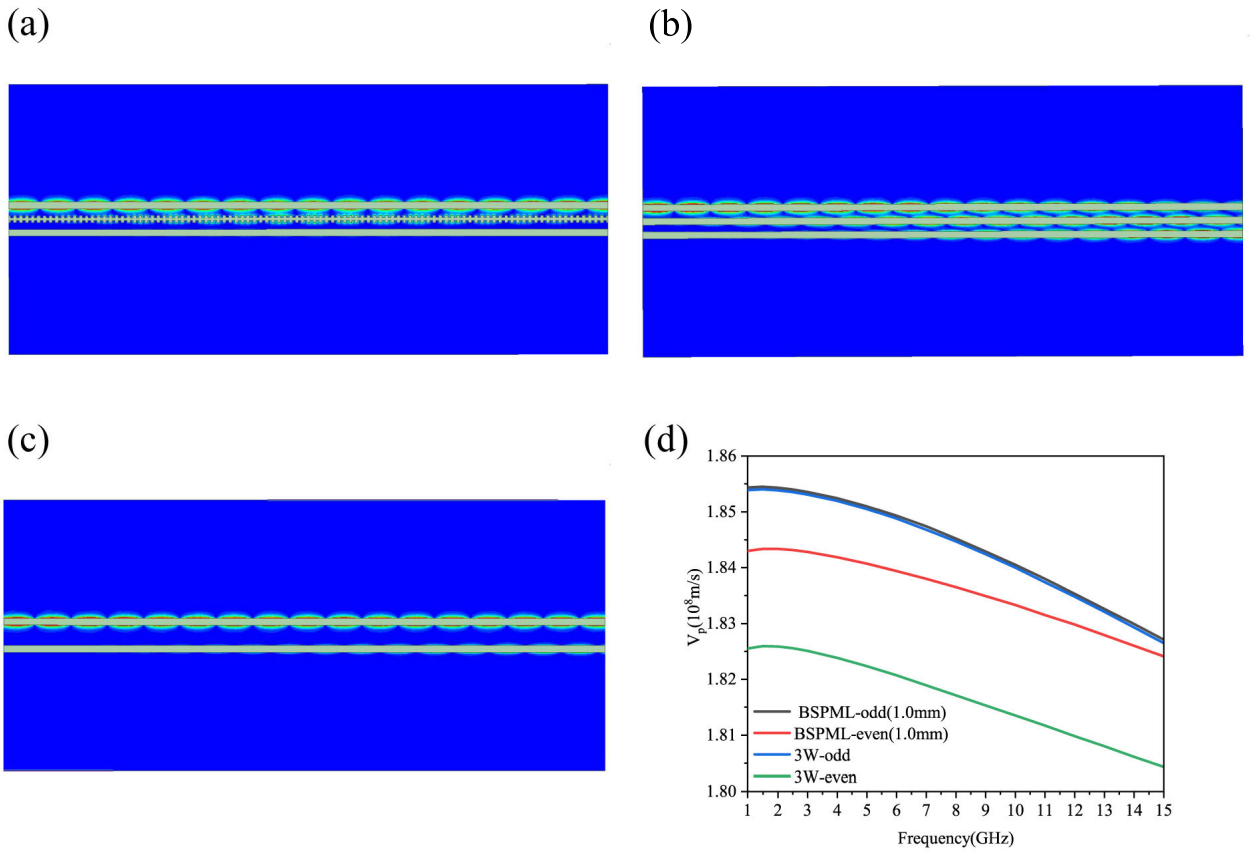

FIGURE 6. The field distribution and phase velocity of the parallel microstrip lines. The field distribution of the parallel microstrip lines isolated by the subwavelength periodic microstrip guard trace and the conventional microstrip guard trace are shown in panels (a) and (b), respectively. The field distribution of the two parallel microstrip lines spaced apart by three times that of the line width is shown in panel (c). The dispersion in the phase velocities of the odd and even modes of the parallel microstrip lines is plotted in panel (d).

microstrip guard trace is about −15 dB. From Table 1, we can clearly understand the numerical results of S_{21} and S_{41} of the four isolation methods at the frequency $f = 15$ GHz. This can be used as a reference for determining which isolation method to be chosen in high-speed circuits. However, under many actual conditions, the front and back ends of guard trace are not allowed to simultaneously connect a resistor, respectively. For example, when the guard trace is applied in the connector region, it is allowed to be connected to one resistor. The initial idea of ours is to dispose a resistor simultaneously at the front and back ends of the subwavelength periodic microstrip lines (in order that the impedance matching is applied to the front and backends), just like having the front and back ends connected to signal sources. However, the difference is that the guard trace will not be connected to any signal sources; hence, the phenomenon is significantly different from the conventional microstrip lines for transmitting signals. In this mechanism, the electromagnetic noise of one conventional microstrip line coupled in the subwavelength periodic microstrip guard trace can be absorbed as much as possible by the front and back resistors in order to reduce the reciprocating oscillation of signals in the guard trace and to avoid resonant coupling. However, in many circuits,

TABLE 1. The results of the simulation of *S*-parameters.

Frequency	Isolation type	S_{21} (dB)	S_{41} (dB)
15GHz	3 W	−1.33	−11.116
15GHz	CML	−12.929	−3.354
15GHz	BSPML (0.5mm)	−1.1056	−18.566
15GHz	BSPML (1.0mm)	−0.9603	−33.971

due to the actual requirement, it is impossible to simultaneously connect two resistors for absorbing the electromagnetic waves at both ends of the subwavelength periodic guard trace. If only one resistor is connected to the subwavelength periodic microstrip guard trace, will the isolation effect be worse? If, however, one resistor is enough to bear complete absorption of the coupled electromagnetic field, and the other end is grounded or unconnected to any devices, then we can ask a question, i.e., whether there will be a resonance effect or not, as suggested in Ref. [13]. Therefore, it is necessary to numerically validate the effect of the present isolating method. In Fig. 5 (c) and (d), we explored the isolation effect on the electromagnetic coupling of the two microstrip lines

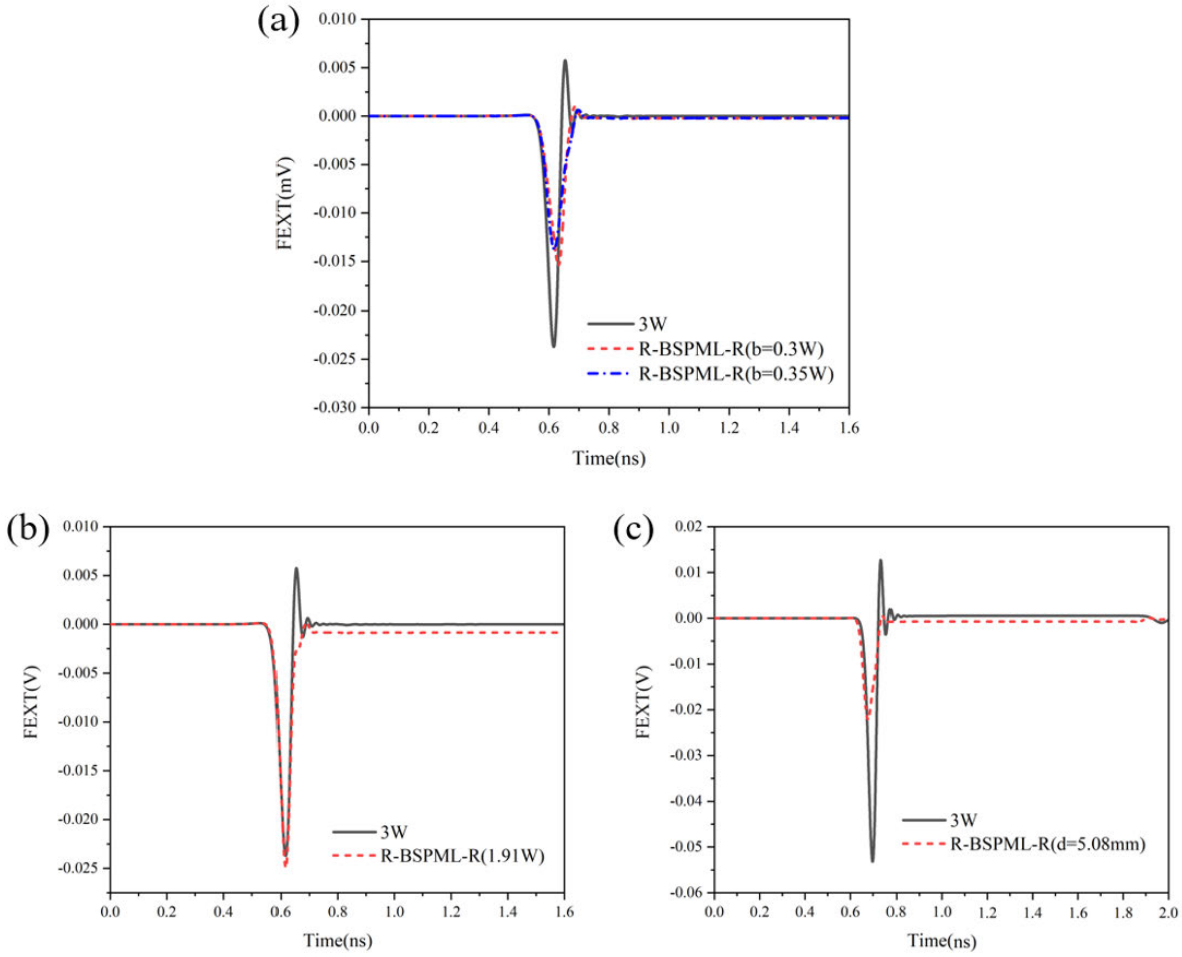

FIGURE 7. Numerical results of far-end crosstalk: (a) the results of structure optimization for the subwavelength periodic microstrip guard trace, (b) the subwavelength periodic microstrip guard trace that can provide the range of circuit area reduction, and (c) the simulation results of FR4 circuit board.

when the subwavelength periodic microstrip guard trace is connected to one resistor only. The subwavelength periodic microstrip guard trace with lattice constant $d = 0.5$ mm was selected to isolate the electromagnetic coupling of the two parallel microstrip lines. It is obvious that the subwavelength periodic microstrip lines connected to one resistor and to two resistors have almost the same isolation effect, and the only difference is that there is a slight jitter in S_{21} and S_{41} curves. The blue line represents the numerical result of S-parameter of the guard trace with one end connected to a resistor and the other end short circuited. The orange line represents the numerical result of S-parameter of the guard trace with one end connected to a resistor and the other end unconnected to any devices. Whether the subwavelength periodic microstrip guard trace with only one resistor in the real circuit can perform its normal function to isolate the electromagnetic interference remains to be verified by experiments. It must be stressed that the S-parameters obtained by the circuit model is highly coincident with the full-wave numerical result in the frequency range under consideration.

According to the field distribution of the parallel microstrip lines in Fig. 6 (a)-(c) and the phase velocities of odd and even modes in Fig. 6 (d), the isolation effect of the subwavelength periodic microstrip guard trace on the EMI between the two parallel microstrip lines can be theoretically understood. The electric field distribution at 15 GHz is considered herein. The electromagnetic coupling between the two parallel microstrip lines is well isolated by the subwavelength periodic microstrip guard trace. It can be found that a part of signals of the conventional microstrip line is coupled to the subwavelength periodic microstrip guard trace, but the field in the subwavelength periodic microstrip guard trace is no longer coupled to another conventional microstrip line. The two parallel microstrip lines have two fundamental modes, i.e., odd and even modes of the coupled microstrip lines. The two modes have different field distributions in the air region, so that they have different phase velocities. The larger the phase velocity difference between the two fundamental modes is, the more the crosstalk between the parallel microstrip lines is. It can be seen in Fig. 6 (d) that the

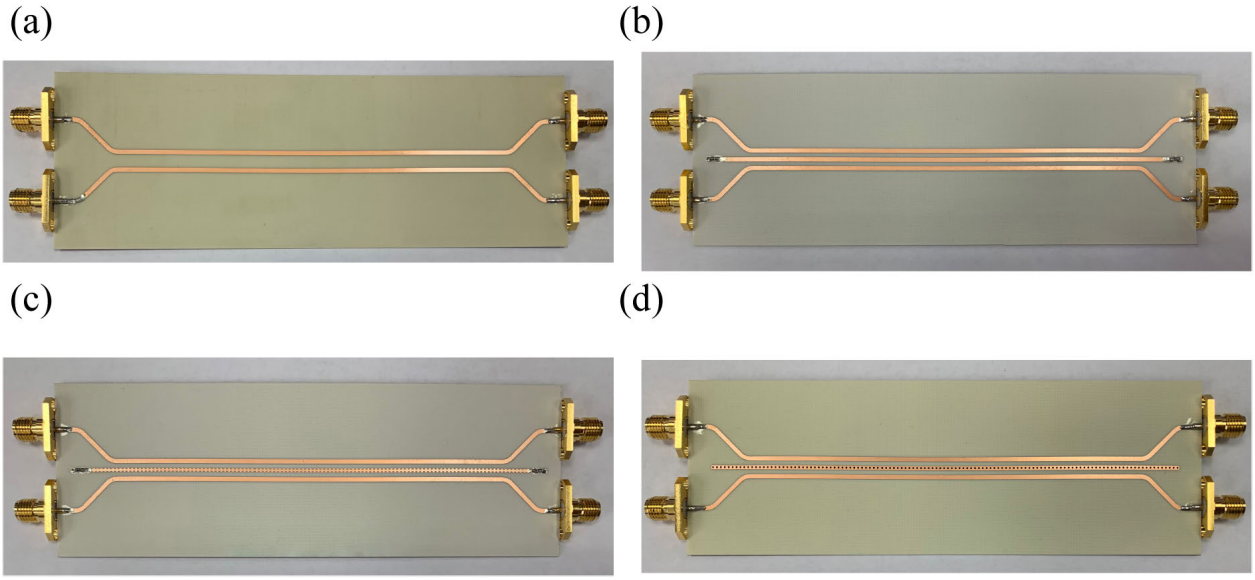

FIGURE 8. The experimental parallel microstrip lines using different types of guard traces for isolating the electromagnetic interference. In panel (a), the two parallel microstrip lines are spaced apart by three times that of the line width; The parallel microstrip lines that are isolated by a conventional microstrip line, a subwavelength periodic microstrip guard trace and a grounded guard trace are shown in panels (b), (c) and (d), respectively.

phase velocity difference between the odd and even modes of the parallel coupled microstrip lines can be reduced by the subwavelength periodic microstrip guard trace in between the two parallel microstrip lines.

Since the subwavelength periodic microstrip guard trace can effectively isolate the far-end crosstalk, we can optimize the structure size of the subwavelength periodic microstrip guard trace. If a step function signal with a rise time of 30 ps and an amplitude of 0.2 V is input from port 1, it is found that when the depth of the groove of the periodic structure is changed from the original $b = 0.3\ w_1$ to $b = 0.35\ w_1$, the simulation results indicate that the far-end crosstalk decreases from the original FEXT peak value of -0.01539 V to -0.01372 V, which is shown in Fig. 7(a). Assuming that the FEXT with the spacing of 3W between the two microstrips is used as the standard, it can be found through the simulation that for the circuit system of the subwavelength periodic microstrip guard line, as shown in Fig. 7(b), the interval between the two microstrip lines can be reduced to 1.91 W. The most practical circuits are composed of multilayer circuit boards, e.g., the FR4 circuit boards have been utilized in most of the practical circuits. We considered the feasibility of employing the subwavelength periodic microstrip guard trace in multilayer FR4 circuit boards for reducing FEXT. In multilayer printed circuit boards, due to the relatively thin thickness of dielectric layer, the width of the microstrip line will be narrow. For example, the thickness of the circuit board dielectric layer analyzed here is 8 mil, the dielectric constant is 4.5, the width of the microstrip line is 14 mil, and the thickness of the metal layer is 0.7 mil, between the two microstrip lines. The spacing between the two microstrip lines is 42 mil, and the total length of the two microstrip lines is 10 cm. The width of the guard trace is $w_1 = 20$ mil, the depth of the groove is $b = 0.35\ w_1$, and the lattice constant is $d = 20$ mil. The FEXT calculated by the full-wave numerical method is shown in Fig. 7(d), where the step function signal with a rise time of 30 ps is input to port 1, and the peak value of the FEXT voltage output by port 4 is -0.04986 V. If a subwavelength period microstrip guard trace is introduced between the two microstrip lines, the peak value of the FEXT output of port 4 is reduced to -0.02588 V. The introduction of the subwavelength periodic microstrip guard trace can make the FEXT decrease by more than 48%. Theoretically, a subwavelength periodic microstrip guard trace designed by systematic simulation would be more feasible than the above structure.

III. EXPERIMENTAL RESULTS

In order to validate the theoretical analysis of the present isolation of EMI caused by the subwavelength periodic microstrip guard trace, an experiment was arranged, where the photos of the circuits to be measured are shown in Fig. 8. Here, the length scale of the main coupled zones of two microstrip lines is 10 cm. The two microstrip lines in the sample shown in Fig. 8 (a) are isolated by three times that of the line width. In Fig. 8 (b)-(d), there are the microstrip circuits, which utilize the conventional microstrip line, the subwavelength periodic microstrip guard trace and the grounded guard trace as their respective shielding wires. The experimental result of the S-parameters of the microstrip circuits is presented in Fig. 9. In the overall measured frequency range as indicated in Fig. 9 (a), the spacing of the two microstrip lines is three times that of the line width, the grounded guard trace and the subwavelength periodic microstrip guard trace

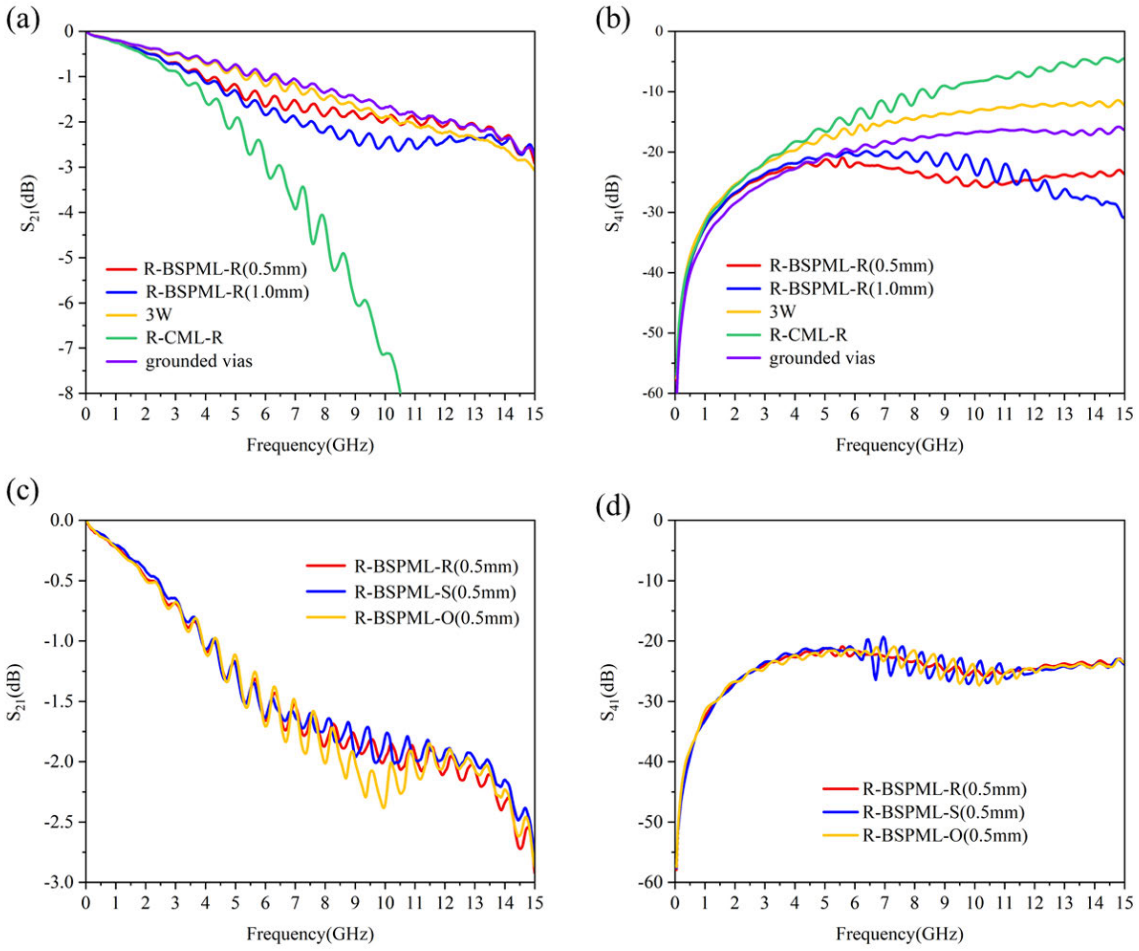

FIGURE 9. The measurement result of the *S*-parameters of the parallel microstrip lines. The dispersion of the parallel microstrip lines of five isolating methods are given in panels (a) and (b). The dispersion of the parallel microstrip lines in the case, where the subwavelength periodic microstrip guard trace is connected to only one resistor, is shown in panel (c) and (d).

can remain S_{21} to be higher than -3 dB in the frequency range under consideration. When the conventional microstrip line is used as a guard trace, S_{21} decreases to -15.863 dB at 15 GHz. Obviously, the conventional microstrip lines are not suitable to the candidate of guard trace, because they have too high a mutual capacitance and a mutual inductance with adjacent microstrip lines. The front and back ends of the subwavelength periodic guard trace are connected to a resistor, respectively. The values of these resistors are not required to be identical with the characteristic impedance of the subwavelength periodic microstrip line. The experimental result in Fig. 9 (a) shows that the isolation effect can be achieved efficiently even if a 50 Ω resistor is used.

If, however, the resistance value deviates excessively from the characteristic impedance of the subwavelength periodic microstrip guard trace, the isolation effect would be reduced. It follows from Fig. 9 (b) that the S_{41} of the subwavelength periodic microstrip guard trace is a little larger than the measurement result of the S_{41} of the grounded guard trace before 4 GHz, but after 4 GHz the S_{41} of the subwavelength periodic microstrip guard trace is much smaller than the measured value of the S_{41} of the grounded guard trace. Therefore, the subwavelength periodic microstrip guard trace can provide a more excellent isolation effect for higher frequency signals. In order that the isolation effect of the subwavelength periodic microstrip guard trace connected to only one resistor can be verified, the lattice constant is chosen as $d = 0.5$ mm of the subwavelength periodic microstrip line. In order to check whether such a design can influence the effect on isolating the electromagnetic signals, three cases for the subwavelength periodic microstrip guard trace are considered: i) two ends connected to resistors, ii) one end connected to a resistor and the other end short circuited, and iii) the other end open circuited. In Fig. 9 (c), the guard trace is connected to only one resistor. The S_{21} of the two guard traces connected to one resistor and to two resistors are slightly different from each other. For example, the S_{21} of the subwavelength periodic microstrip guard trace with one end connected to a resistor and one end open circuited in 8-11 GHz is a little lower than that of the guard trace with two ends connected to

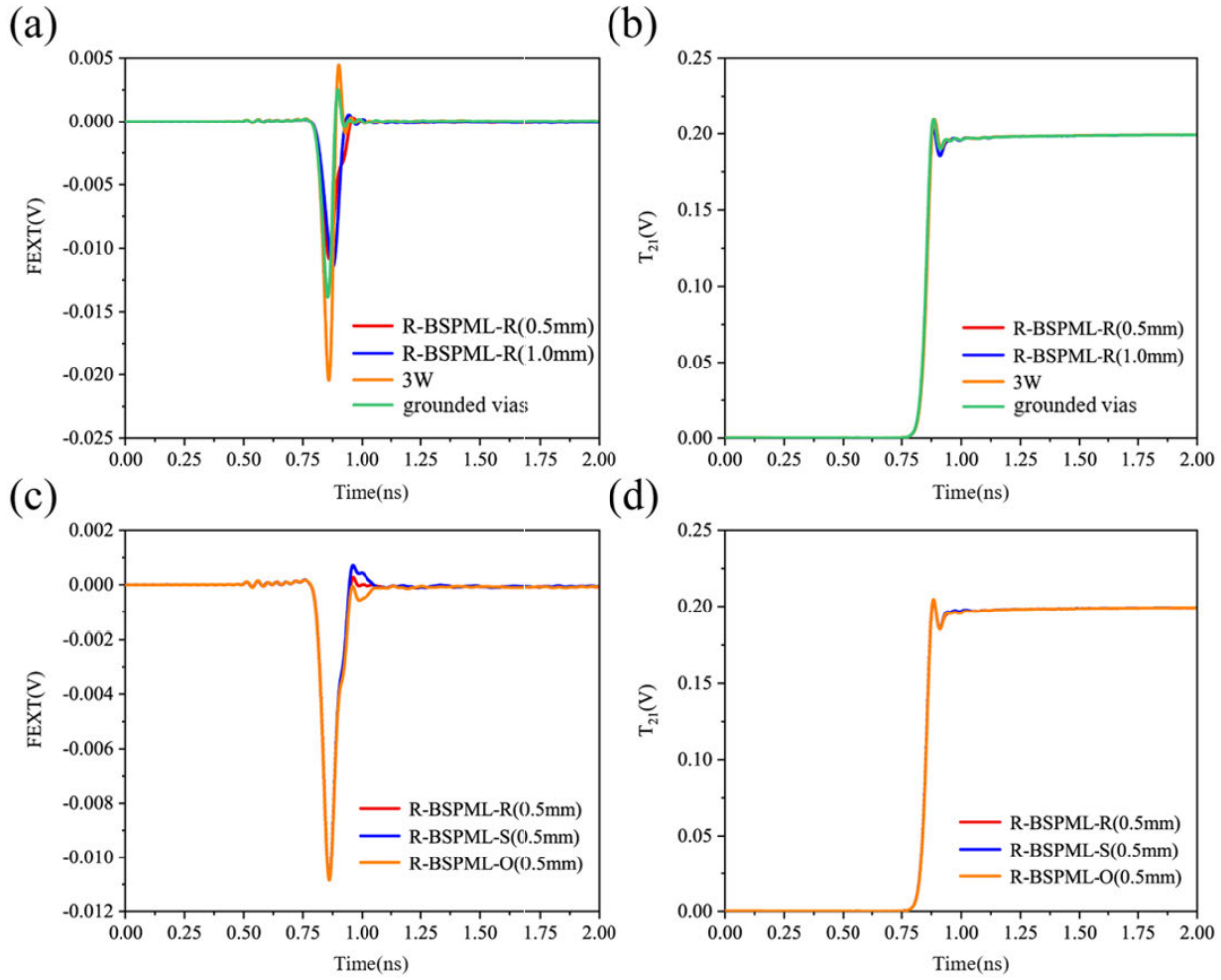

FIGURE 10. The time-domain signal measurement results. The far-end crosstalk measurement result of the parallel microstrip lines in four isolating methods is shown in panel (a) and the output step function signal of the parallel microstrip lines isolated by the guard trace is given in panel (b); The far-end crosstalk measurement result and the output step function signal of the parallel microstrip lines isolated by the subwavelength periodic microstrip guard trace connected to only one resistor are plotted in panels (c) and (d), respectively.

two resistors. The blue line in Fig. 9 (c) represents the S_{21} measurement result of the guard trace with one end connected to a resistor and the other end short circuited, and the orange line represents the S_{21} measurement result of the guard trace with one end connected to a resistor and the other end unconnected to any devices. The S_{41} measurement result of the guard trace connected to only one resistor is given in Fig. 9 (d). It can be shown that the guard trace connected to only one resistor has slight jitters at 6-11 GHz and the rest is slightly different from the measurement result of the guard trace with both ends connected to resistors. Table 2 shows the measurement results of S-parameters at 15 GHz. Our time-domain signal measurement results are shown in Fig. 10. In Fig. 10 (a), which is the FEXT measurement result, a step function signal of 30 ps rise time and 0.2 V amplitude is imported into Port 1, and the FEXT can be measured at Port 4. For the microstrip lines spaced apart by three times that of the line width, the maximum amplitude of FEXT is -0.02046 V, about 10% of the input signal amplitude.

TABLE 2. The results of the measurement of S-parameters.

Frequency	Isolation type	S_{21} (dB)	S_{41} (dB)
15GHz	3 W	-3.076	-12.293
15GHz	CML	-15.863	-4.481
15GHz	BSPML (0.5mm)	-2.923	-23.686
15GHz	BSPML (1.0mm)	-2.768	-30.853

The FEXT is changed to -0.01384 V by the grounded guard trace, about 7% of the input signal amplitude. The amplitude of FEXT of the subwavelength periodic microstrip guard trace with $d = 1.0$ mm is -0.01143 V. The amplitude of FEXT of the subwavelength periodic microstrip guard trace with $d = 0.5$ mm is -0.01078 V, about 5% of the input signal amplitude. The subwavelength periodic guard trace with a lattice constant of $d = 0.5$ mm can almost meet the requirement for 5% crosstalk noise. It is observed that the

TABLE 3. Experimental measurement results of far-end crosstalk.

Rise time (ps)	Input signal (V)	Isolation type	Peak of FEXT (V)
30	0.2	3 W	−0.02046
30	0.2	grounded vias	−0.01384
30	0.2	BSPML(0.5mm)	−0.01078
30	0.2	BSPML(1.0mm)	−0.01143

conventional grounded guard trace reduces the crosstalk by only 32%. But our technique can reduce the crosstalk by 50%. Obviously, the FEXT can be efficiently controllable by modifying the geometric dimension of the periodic guard trace in the allowable noise range of the circuit system. In fact, in order that the measured value of FEXT can be dramatically reduced, the slot depth b should be increased, while the lattice constant d should become smaller, i.e., an optimized structure can be achieved through systematic simulation. In Fig. 10 (b), where the output step function signals of port 2 is shown, the output signals of the four isolating methods are almost overlapped. It is pointed out that in the four cases of isolating methods, the signal rise times are given by 46.4735 ps for the parallel microstrip lines (spaced apart by three times that of the line width), 45.448 ps for the grounded guard trace, 46.4735 ps for the subwavelength periodic microstrip guard trace with the lattice constant $d = 1.0$ mm, and 46.1318 ps for the subwavelength periodic microstrip guard trace with the lattice constant $d = 0.5$ mm. In a word, the four isolation structures have slight differences in the rise time of the T_{21} output signals. Fig. 10 (c) shows the FEXT when the subwavelength periodic microstrip guard trace is connected to only one resistor. It can be observed that the difference in FEXT of the subwavelength periodic microstrip guard traces connected to one resistor and to two resistors is very slight. In the three isolating methods shown in Fig. 10 (d), where the output step function signals of port 2 are given, it can be found that the signal outputs are almost the same for the guard traces that are connected to one resistor and to two resistors. Here, the FEXT peak results of the four FEXT isolation schemes are listed in Table 3.

The current high-speed or high-frequency circuit boards have a lot of grounded holes for isolating crosstalk. Generally, the electromagnetic interference between shielding wires is isolated by grounded holes; however, as the PCB has a lot of grounded holes, the wiring of a multilayer printed circuit board becomes difficult. Since the present novel guard trace has only one grounded hole, it almost does not affect the design of a multilayer printed circuit board.

When the rise time of the digital signal becomes shorter, it is no longer enough to keep three times the line width between the two microstrip lines to meet the requirements of the circuit system for far-end crosstalk. Then it is necessary to adopt a suitable isolation structure to reduce the crosstalk between the microstrip lines. The commonly used isolation method is that the two microstrip lines are separated by 3 times the line width and a grounded guard trace is introduced in the middle. Since a large number of high-density grounded holes need to be introduced for the grounded guard trace, if these grounded holes penetrate the multilayer printed circuit board, the second layer PCB routing will face unimaginable difficulties and reduce the yield of the board. Our isolation method requires only one grounded via hole, and so the production yield of the board can be improved. With HDI technology, grounded holes that do not penetrate the circuit board will not affect the design of the second-layer circuit board, which can increase the signal transmission rate and effectively use the space of each layer of circuit board. However, it will still face the problems caused by the existence of a large number of grounded holes. Our technology can also make use of HDI technology, and only one grounded hole is required, which improves the production yield of the circuit board. The introduction of grounded holes on the surface of the circuit board requires a lot of additional processing costs. Usually when HDI is used, the technology will increase the manufacturing cost of the circuit board by more than 30%. With the flexibility of the size of the subwavelength periodic microstrip guard line, the percentage of the FEXT voltage amplitude can be smaller than the system tolerance. However, if you really want to utilize new technology to isolate FEXT, the structure size of such subwavelength periodic guard traces often needs to be optimized in order to obtain the satisfactory results. However, whether the grounded guard trace or the subwavelength periodic guard trace to isolate crosstalk is used, the two microstrips space must be reserved between the lines to place the guard traces, which is not conducive to the miniaturization of the circuit area.

IV. CONCLUSION

A new scenario of three guard traces based on a subwavelength periodic microstrip line to isolate the EMI between two parallel microstrip lines has been proposed in this work. We suggested three guard traces corresponding to three cases: In the first case, each of the two ends of the subwavelength periodic microstrip line is connected to a resistor. In the second case, one end of the subwavelength periodic microstrip line is connected to a resistor, and the other end is connected to a metal cylinder which is grounded or ungrounded. In the third case, one end is connected to a resistor, and the other end is connected to nothing. Therefore, in some applications, the present novel guard trace has only one grounded hole, whereas the conventional grounded guard trace has a lot of

grounded holes, which severely influence the circuit layout on a multilayer board. In order to study the isolation effect of subwavelength periodic microstrip guard trace on electromagnetic signals, the circuit parameters (including mutual capacitance and mutual inductance) of circuit systems with a guard trace were calculated by using the numerical method, and a complete circuit model was built, so the present numerical simulation of circuit systems can be directly performed in a SPICE simulator. It was shown in the theoretical and experimental results that this guard trace can dramatically reduce the mutual capacitance and mutual inductance of the overall circuit system, meaning the EMI between transmission lines can be reduced. For the digital signals of 30 ps rise time, the guard trace based on subwavelength periodic microstrip line can suppress the FEXT almost below 5% of transmission signal amplitude when the spacing between two microstrip lines is triple line width, so that it can be employed in actual circuit systems.

ACKNOWLEDGMENT

The authors would like to thank Prof. Song-Tsuen Peng (National Chiao-Tung University, Taiwan), Prof. Yu-Shan Li (Xidian University, Xi'an), Prof. Hai-Hui Zha and Prof. Hao Feng (Keysight Company Ltd., Shanghai), and Prof. Lei Shi (Ceyear Techologies Company Ltd., Qingdao) for their helpful discussions, and also would like to thank Prof. Jianqing Shi and Prof. Qiang Lin for helping establishing the Microwave Measurement Laboratory.

REFERENCES

[1] J.-J. Wu, "Subwavelength microwave guiding by periodically corrugated strip line," *Prog. Electromagn. Res.*, vol. 104, pp. 113–123, 2010.
[2] D. J. Hou, J.-J. Wu, C.-J. Wu, J. Q. Shen, H.-L. Chiueh, L.-Y. Cheng, and H.-E. Lin, "Experimental measure of transmission characteristics of low-frequency surface plasmon polaritons in frequency and time domains," *Opt. Exp.*, vol. 24, no. 7, pp. 7387–7397, 2016.
[3] E. Bogatin, *Signal and Power Integrity-Simplified*, 2nd ed. Upper Saddle River, NJ, USA: Prentice-Hall, 2009, pp. 475–553.
[4] F. Xiao, W. Liu, and Y. Kami, "Analysis of crosstalk between finite-length microstrip lines: FDTD approach and circuit-concept modeling," *IEEE Trans. Electromagn. Compat.*, vol. 43, no. 4, pp. 573–578, Nov. 2001.
[5] D. A. Hill, K. H. Cavcey, and R. T. Johnk, "Crosstalk between microstrip transmission lines," *IEEE Trans. Electromagn. Compat.*, vol. 36, no. 4, pp. 314–321, Nov. 1994.
[6] F. D. Mbairi, W. P. Siebert, and H. Hesselbom, "High-frequency transmission lines crosstalk reduction using spacing rules," *IEEE Trans. Compon. Packag. Technol.*, vol. 31, no. 3, pp. 601–610, Sep. 2008.
[7] B.-R. Huang, K. C. Chen, and C. L. Wang, "Far-end crosstalk noise reduction using decoupling capacitor," *IEEE Trans. Electromagn. Compat.*, vol. 58, no. 3, pp. 836–848, Jun. 2016.
[8] L. Tani and N. El Ouazzani, "Minimizing crosstalk on printed circuit board using non uniform guard traces," in *Proc. Int. Conf. Inf. Technol. Organizations Develop. (IT4OD)*, Fez, Morocco, Mar. 2016, pp. 1–4.
[9] D. N. Ladd and G. L. Gostache, "SPICE simulation used to characterize the cross-talk reduction effect of additional tracks grounded with vias on printed circuit boards," *IEEE Trans. Circuits Syst. II, Analog Digit. Signal Process.*, vol. 39, no. 2, pp. 342–347, Jun. 1992.
[10] S. Li, Y. Liu, Z. Song, and H. Hu, "Analysis of crosstalk of coupled transmission lines by inserting additional traces grounded with vias on printed circuit boards," in *Proc. Asia–Pacific Conf. Environ. Electromagn. (CEEM)*, Hangzhou, China, Nov. 2003, pp. 451–454.
[11] L. Zhi, W. Qiang, and S. Changsheng, "Application of guard traces with vias in the RF PCB layout," in *Proc. 3rd Int. Symp. Electromagn. Compat.*, Beijing, China, 2002, pp. 771–774.
[12] W.-T. Huang, C.-H. Lu, and D.-B. Lin, "Suppression of crosstalk using serpentine guard trace vias," *Prog. Electromagn. Res.*, vol. 109, pp. 37–61, 2010.
[13] A. Suntives, A. Khajooeizadeh, and R. Abhari, "Using via fences for crosstalk reduction in PCB circuits," in *Proc. IEEE Int. Symp. Electromagn. Compat. (EMC)*, Portland, OR, USA, Aug. 2006, pp. 34–37.
[14] G.-H. Shiue, C.-Y. Chao, and R.-B. Wu, "Guard trace design for improvement on transient waveforms and eye diagrams of serpentine delay lines," *IEEE Trans. Adv. Packag.*, vol. 33, no. 4, pp. 1051–1060, Nov. 2010.
[15] F. D. Mbairi, W. P. Siebert, and H. Hesselbom, "On The problem of using guard traces for high frequency differential lines crosstalk reduction," *IEEE Trans. Compon. Packag. technol.*, vol. 30, no. 1, pp. 67–74, Mar. 2007.
[16] S. T. Peng, T. Tamir, and H. L. Bertoni, "Theory of dielectric waveguide," *IEEE Trans. Microw. Theory Techn.*, vol. 23, no. 1, pp. 123–133, Jan. 1975.
[17] J. J. Wu, "An equivalent network method for the analysis of nonuniform period structures," *Microw. Opt. Technol. Lett.*, vol. 15, no. 3, pp. 149–153, Jun. 1997.
[18] T. Tamir, *Integrated Optics: Topics in Applied Physics*. Berlin, Germany: Prentice-Hall, 1979.
[19] A. A. Oliner, *Antenna Engineering Handbooks*, 4th ed. New York, NY, USA: McGraw-Hill, 2007.
[20] J. B. Pendry, L. Martín-Moreno, and F. J. Garcia-Vidal, "Mimicking surface plasmons with structured surfaces," *Science*, vol. 305, no. 5685, pp. 847–848, Aug. 2004.
[21] S. K. Lee, K. Lee, H. J. Park, and J. Y. Sim, "FEXT-eliminated stub-alternated microstrip line for multi-gigabit/second parallel links," *Electron. Lett.*, vol. 44, no. 4, pp. 272–273, Feb. 2008.
[22] J. J. Wu, D. C. Tsai, T. J. Yang, H. E. Lin, H. L. Chiueh, L. Shen, I. J. Hsieh, J. Q. Shen, W. O. Yang, and Z. Gao, "Reduction of wide-band crosstalk for guiding microwave in corrugated metal strip lines with subwavelength periodic hairpin slits," *IET Microw., Antennas Propag.*, vol. 6, no. 2, pp. 231–237, Feb. 2012.
[23] X. Shen, T. J. Cui, D. F. Martin-Cano, and J. Garcia-Vidal, "Conformal surface plasmons propagating on ultrathin and flexible films," *Proc. Nat. Acad. Sci. USA*, vol. 110, no. 1, pp. 40–45, Jan. 2013.
[24] S. Zhao, H. C. Zhang, L. Liu, J. Zhao, and C. Yang, "A novel low-crosstalk driveline based on spoof surface plasmon polaritons," *IEEE Access*, vol. 7, pp. 30702–30707, 2019.
[25] J. J. Wu, D. J. Hou, K. Liu, L. Shen, C. A. Tsai, C. J. Wu, D. Tsai, and T.-J. Yang, "Differential microstrip lines with reduced crosstalk and common mode effect based on spoof surface plasmon polaritons," *Opt. Exp.*, vol. 22, no. 22, pp. 26777–26787, 2014.
[26] C. H. Wu, G. Zhou, J.-Y. Juang, Q. Shen, Y. You, J. Yan, L. Shen, H. Zhang, Y. Wu, F. Zhu, and C. C. Chang, "Circuit model of parallel corrugated transmission lines for differential signal propagating in microwave band," *IEEE Access*, vol. 8, pp. 221783–221793, 2020.
[27] X. Dai, W. Feng, and W. Che, "Reduction of UWB far-end crosstalk in microwave and millimeter-wave band of parallel periodically loaded transmission lines with discontinuous structured guard lines," *IEEE Trans. Plasma Sci.*, vol. 48, no. 7, pp. 2372–2383, Jul. 2020.
[28] C. R. Paul, *Analysis of Multi-Conductor Transmission Lines*, 2nd ed. Hoboken, NJ, USA: Wiley, 2005, pp. 18–19.
[29] R. E. Collin, *Foundation for Microwave Engineering*, 2nd ed. New York, NY, USA: McGraw-Hill, 1992, pp. 550–551.

CHIA HO WU was born in Tainan, Taiwan. He received the M.S. degree in physics from the National Tsing Hua University, Hsinchu, Taiwan, in 1987, and the Ph.D. degree in electro-optics from Chiao Tung University, Hsinchu, in 1997. He has been a Professor with the Department of Applied Physics, College of Science, Zhejiang University of Technology, Hangzhou, China, since 2018. His research interests include propagation and scattering of dielectric waveguides, numerical analysis of dielectric gratings, active leaky wave antennas, and subwavelength periodic metal structures.

PEIXUN MA was born in Fuyang, Anhui, China, in 1997. He received the B.S. degree from the Anhui University of Technology, Anhui, in 2019. He is currently pursuing the master's degree with the Zhejiang University of Technology. His research interests include microwave, millimeter-wave, and subwavelength periodic structures.

GUOBING ZHOU was born in Huzhou, Zhejiang, China, in 1994. He received the B.S. degree from the Zhejiang University of Technology, Zhejiang, in 2017, where he is currently pursuing the master's degree. His research interests include microwave, millimeter-wave, and subwavelength periodic structures.

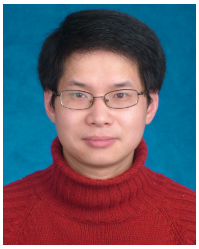

JIANQI SHEN was born in Hangzhou, Xiaoshan, Zhejiang, China, in November 1974. He received the joint Ph.D. degree from the Joint Research Centre of Photonics, Royal Institute of Technology, Sweden, and Zhejiang University, China. Then, he did his postdoctoral research with Zhejiang University, from 2006 to 2008. He is currently an Associate Professor with the College of Optical Science and Engineering, Zhejiang University. His research interests include surface plasmonics, electromagnetic metamaterials, quantum optics, and related theoretical topics in classical and quantum field theories.

ZHENYU QIAN was born in Ningbo, Zhejiang, China, in 2000. She is a senior majoring in optoelectronic information science and engineering with the Zhejiang University of Technology and will work towards a master's degree in this university in September. Her research interests include metamaterials, crosstalk analysis of high-speed signal, and antenna design.

LINFANG SHEN was born in Zhejiang, China, in 1965. He received the B.S. degree in physics from Peking University, Beijing, China, in 1986, the M.S. degree in plasma physics from the Institute of Plasma Physics, Academy of Science of China, Hefei, China, in 1989, and the Ph.D. degree in electronic engineering from the University of Science and Technology of China, in 2000. He is currently a Professor with the Zhejiang University of Technology. His present research interests include surface plasmonics, photonic crystals, and metamaterials.

HANG ZHANG was born in Zhejiang, China. He received the Ph.D. degree in physics from Zhejiang University, Hangzhou, China, in 2002. He is currently an Associate Professor with the Department of Applied Physics, College of Science, Zhejiang University of Technology. His research interests include free form optical design, semiconductor illumination, and the propagation of subwavelength periodic metal structures.

ZHUOYUAN WANG is currently a Professor with the Electronic and Information Engineering College, Ningbo University of Technology. He majored in electronic science and technology with Zhejiang University. He is mainly engaged in electromagnetic field theory, metamaterials, electromagnetic structure design, RF device design, and optimization. He has undertaken two projects of Natural Science Foundation of Zhejiang Province and several projects of Natural Science Foundation of Ningbo. He has published more than 20 professional papers.

XIAOLONG WANG was born in Qingdao, China. He received the B.S. degree in physics from Zhejiang University, in 2006, the Ph.D. degree in optics from Zhejiang University, and the Ph.D. degree in physics from Paris Observatory, in 2011, by following agreements between ministries of education of China and France. Since 2014, he has been working as an Assistant Professor with the College of Science, Zhejiang University of Technology. His research interests include atom interferometry, optical spectroscopy, and metamaterials.

FANG HE (Senior Member, IEEE) received the B.Eng. degree in communication engineering from Jilin University, Changchun, China, in 2002, and the M.Sc. degree in communication engineering and the Ph.D. degree in electrical and electronics engineering from The University of Manchester, Manchester, U.K., in 2005 and 2011 respectively. He had been with HellermannTyton Data Ltd., Northampton, U.K., since 2009, where he was the Product Development Engineer. Since 2019, he has been with Zhejiang Zhaolong Interconnect Technology Company Ltd., Deqing, China, where he is currently the Chief Specialist of Generic Cabling and the Laboratory Director. He is a member of Institution of Engineering and Technology (IET), U.K. He is also a Chartered Engineer from the Engineering Council, U.K.